Journal of Power Sources 195 (2010) 8209–8214

Contents lists available at ScienceDirect

Journal of Power Sources

journal homepage: www.elsevier.com/locate/jpowsour

Co–SiO_2 nanosphere-catalyzed hydrolytic dehydrogenation of ammonia borane for chemical hydrogen storage

Tetsuo Umegaki, Jun-Min Yan, Xin-Bo Zhang, Hiroshi Shioyama, Nobuhiro Kuriyama, Qiang Xu*

National Institute of Advanced Industrial Science and Technology (AIST), 1-8-31 Midorigaoka, Ikeda, Osaka 563-8577, Japan

ARTICLE INFO

Article history:
Received 11 March 2010
Received in revised form 15 July 2010
Accepted 21 July 2010
Available online 30 July 2010

Keywords:
Cobalt clusters
Hydrolysis
Ammonia borane
Hydrogen generation

ABSTRACT

Cobalt clusters–silica nanospheres (15–30 nm) were synthesized using a $Co(NH_3)_6Cl_3$ template method in a polyoxyethylene-nonylphenyl ether/cyclohexane reversed micelle system followed by in situ reduction in aqueous $NaBH_4/NH_3BH_3$ solutions. The cobalt clusters are located either inside or on the outer surface of the silica nanospheres as shown by the transmission electron microscope (TEM)/energy dispersive X-ray (EDX) and X-ray photoelectron spectroscopy (XPS) measurements. The cobalt–silica nanospheres have a high catalytic activity for the hydrolysis of ammonia borane that generates a stoichiometric amount of hydrogen, and can be efficiently cycled and reused 10 times without any significant loss of the catalytic activity.

1. Introduction

Interest in hydrogen as an energy carrier for wide-spread use has dramatically grown. The application of hydrogen fuel cells to portable power sources requires a compact and lightweight hydrogen storage or on-board hydrogen generation based on the rapid and efficient energy conversion of a convenient and inexpensive hydrogen source. Although many efforts have contributed to the development of hydrogen-storage materials [1,2] and on-board reforming of hydrocarbons into hydrogen [3], further advances in hydrogen-storage and hydrogen-production technologies must be made if a hydrogen-based energy system is to be established. One of the main challenges for the development of hydrogen-storage materials is to improve the volumetric/gravimetric capacities. For the on-board reforming, the high system operating temperature poses an obstacle to its practical application. Boron- and nitrogen-based chemical hydrides, such as $LiNH_2$–LiH [4] and $NaBH_4$ [5,6], are the preferred hydrogen carriers for PEM fuel cells because of their relatively high hydrogen capacities [7]. Ammonia borane, NH_3BH_3, has become an attractive and feasible candidate for chemical hydrogen-storage applications due to its combination of low molecular weight (30.7 g mol^{-1}) and high gravimetric hydrogen capacity (19.6 wt.%). Intensive efforts have been made to enhance the kinetics of the hydrogen release from this compound from both solid [8,17] and solution approaches [9–31].

A system based on the transition metal-catalyzed dissociation and hydrolysis of NH_3BH_3 has been achieved that releases hydrogen at room temperature [11,13–31]. NH_3BH_3 dissolves in water to form a solution stable in the absence of air. The addition of a catalytic amount of suitable metal catalysts into the solution leads to the rapid release of hydrogen gas with an H_2 to NH_3BH_3 ratio up to 3.0. Not only noble metals, such as Pt [11,14], Ru [11,14,15,18], and Rh [11,14–17], but also non-noble metal-based catalysts, such as Co [13,15,16,26,30], Ni [13,15,21,22,27], and Fe [13,20], have been found to be effective for accelerating this reaction. This hydrogen generation system possesses a high potential for application in portable fuel cells. For practical use, low-cost and high performance non-noble metal catalysts are desired. Investigations of the catalysts required for hydrogen generation from an aqueous NH_3BH_3 solution have suggested that the catalytic activity depends on the dispersion of the active metals [13,14,17,20,22–25,27,30]. However, few publications have reported the effect of dispersion of the active phase of cobalt catalysts on the catalytic performance and the recycling for the hydrolysis of NH_3BH_3.

Interests in nanoparticles or nanoclusters coating with spherical silica or within the silica spheres have been growing due to their potential utilities in photonics [32–36], magnetics [37], catalysis [25,38–42,44], and absorbents [43–45]. The preparation of nanoparticles or nanoclusters prepared in a reverse micelle system has received considerable attention due to the possibility to obtain mono-dispersed particles of nanometer size [33,35–45]. Metal clusters in silica nanospheres were successfully synthesized using the crystal template method with metal ammine complexes in the hexaoxyethylene-nonylphenyl ether

* Corresponding author. Tel.: +81 72 751 9562; fax: +81 72 751 7942.
E-mail address: q.xu@aist.go.jp (Q. Xu).

0378-7753/$ – see front matter © 2010 Elsevier B.V. All rights reserved.
doi:10.1016/j.jpowsour.2010.07.079

(NP-6)/cyclohexane reversed micelle system [43–45]. We also successfully synthesized nickel clusters contained within silica nanospheres (20–30 nm) using a $Ni(NH_3)_6Cl_2$ crystal template in a polyoxyethylene-nonylphenyl ether/cyclohexane reversed micelle system followed by in situ reduction in an aqueous $NaBH_4/NH_3BH_3$ solution [22]. The nickel–silica nanospheres show a higher catalytic activity for the hydrolysis of ammonia borane that generates a stoichiometric amount of hydrogen than the silica supported nickel catalysts.

The present paper reports that cobalt–silica nanospheres exhibit a high catalytic activity and excellent durability for hydrogen generation by the hydrolysis of ammonia borane..

2. Experimental

2.1. Catalyst preparation

$Co–SiO_2$ nanospheres were prepared by the following reversed micelle techniques. An aqueous hexaamminecobalt chloride ($Co(NH_3)_6Cl_3$, Mitsuwa Chem. Co., >99.0%) solution (3.6 mL) was rapidly added to 800 mL of NOIGEN EA-80 (polyoxyethylene-nonylphenyl ether; supplied by Daiichi Kogyo Seiyaku Co.) cyclohexane (Kishida Chem. Co., >99.5%) solution. The concentrations of $Co(NH_3)_6Cl_3$ were 160 mM, which determined that the Co contents of the products $Co/(Co + SiO_2) = 8.3$ wt.%. After stirring at room temperature for 12 h, 3.6 mL of a 28 wt.% aqueous ammonia solution (Kishida Chem. Co.) was rapidly added, and after 2 h, 1.39 mL of tetraethoxysilane ($Si(OC_2H_5)_4$, Kishida Chem. Co., >99.0%) was rapidly added. The solution was initially transparent, but became slightly cloudy after 2 days of stirring. The resulting solution was phase separated by the addition of methyl alcohol (Kishida Chem. Co., 99.8%), followed by filtration and washing with cyclohexane and acetone (Kishida Chem. Co., >99.5%). After drying in a desiccator overnight, the obtained orange fine powders were evacuated at 573 K for 5 h.

The SiO_2 supported Co catalysts used in this study were prepared by the conventional impregnation method. SiO_2 prepared similar to the preparation of the $Co–SiO_2$ nanospheres (without evacuation treatment) was used as the catalytic support. For preparing the SiO_2 supported catalysts, impregnation was performed by evaporating the SiO_2 support with an aqueous $Co(NH_3)_6Cl_3$ solution at 303 K, and the obtained powders were evacuated at 573 K for 5 h.

2.2. Characterization

Powder X-ray diffraction (XRD) was performed by a RINT-2200 X-ray diffractometer with a Cu Kα source (40 kV, 40 mA) for the $Co–SiO_2$ nanospheres and the SiO_2 supported Co catalysts. The catalysts were held on a glass substrate and covered by an adhesive tape on the surface to minimize the sample exposure to oxygen and moisture during the measurement.

The morphologies of the $Co–SiO_2$ nanospheres and the SiO_2 supported Co catalyst were observed using a Tecnai G^2 20 Twin transmission electron microscope (TEM) operating with an acceleration voltage of 200 kV, which was also equipped with a CCD camera (Gatan Image Filter) and an energy dispersive X-ray detector (EDX).

X-ray photoelectron spectra were acquired using an ESCA-3400 spectrometer (Simadzu Corp.) equipped with a Mg Kα X-ray excitation source (1253.6 eV) operating at 10 kV and 10 mA. The binding energies (BE) were referred to the C 1s peak at 285.0 eV. After the initial data were collected, a 2 kV Ar^+ sputter beam was used for depth profiling of the samples before and after the hydrolysis of NH_3BH_3.

The ICP analyses of the reaction mixtures after centrifugal separation of the catalysts were performed by a CIROS-120 EOP Inductively Coupled Plasma (ICP) spectrophotometer (Rigaku Corp.).

2.3. Experimental procedures for hydrolysis of ammonia borane

A mixture of sodium borohydride ($NaBH_4$, 10 mg, Aldrich, >98.5%), ammonia borane (NH_3BH_3, 50 mg, Aldrich, 90%), and catalyst was kept in a two-necked round-bottom flask. One neck was connected to a gas burette, and the other was connected to a pressure-equalization funnel used to introduce the distilled water (10 mL). The reaction started when the distilled water was added to the mixture of $NaBH_4$, NH_3BH_3, and the catalyst, and the evolution of gas was monitored using the gas burette. The reactions were carried out at room temperature in air.

After the hydrogen generation reaction was completed, a further aliquot of the aqueous NH_3BH_3 solution (0.16 M, 10 mL) was subsequently added to the reaction flask and the evolution of gas was monitored using the gas burette. Such cycle tests of the catalyst for the hydrolysis of NH_3BH_3 were carried out 10 times.

All the samples after the reaction were centrifugally separated from the reaction solution, and then dried in a desiccator under vacuum conditions.

3. Results and discussion

Fig. 1a and b shows the time courses of the hydrogen evolution from the aqueous NH_3BH_3 and $NaBH_4$ solution using the un-reduced samples of $Co–SiO_2$ nanospheres and the SiO_2 supported Co catalyst. The reaction rate significantly depends on the catalysts. The evolutions of 135 and 140 mL of hydrogen were finished in 14 and 5 min in the presence of the $Co–SiO_2$ nanospheres and the SiO_2 supported Co catalyst, respectively. As shown in Fig. 1c, only a negligible amount of hydrogen is generated without adding $NaBH_4$ to the $Co–SiO_2$ nanospheres and NH_3BH_3. The result suggests that $NaBH_4$ is necessary to activate the catalysts. The effect of $NaBH_4$ has been reported on $Ni–SiO_2$ nanospheres for the hydrolysis of NH_3BH_3 [25]. In the present reaction system using

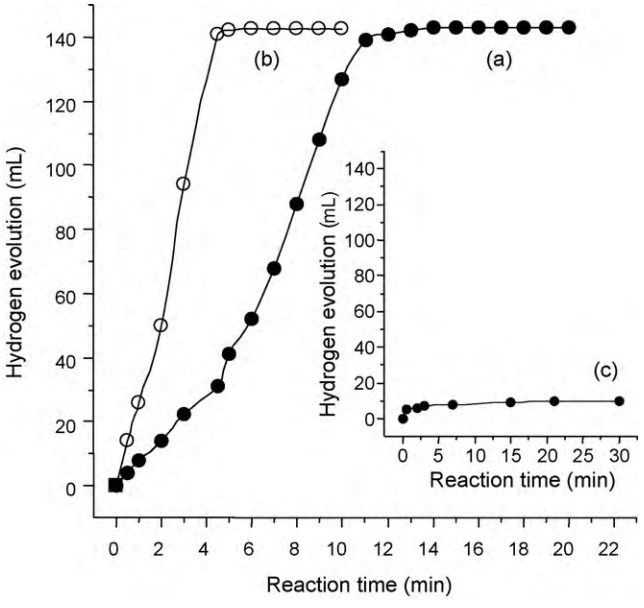

Fig. 1. Hydrogen generation by the hydrolysis from aqueous NH_3BH_3 (50 mg) and $NaBH_4$ (10 mg) solution (10 mL) in the presence of (a) the $Co–SiO_2$ nanospheres, (b) the SiO_2 nanospheres supported Co catalyst with and (c) without adding $NaBH_4$ to the $Co–SiO_2$ nanospheres. $Co/NH_3BH_3 = 0.05$.

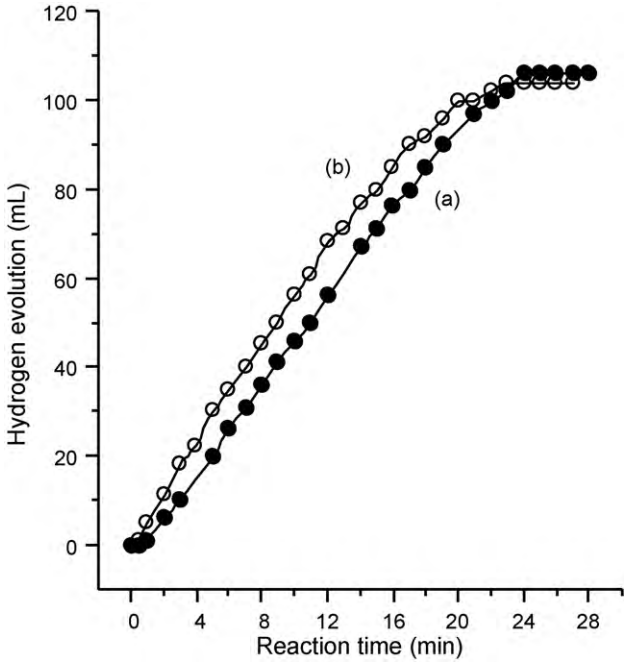

Fig. 2. Hydrogen generation from aqueous NH_3BH_3 solution in the presence of the reduced samples of (a) the Co–SiO_2 nanospheres and (b) the SiO_2 nanospheres supported Co catalyst at the 1st cycle of use (after the reaction in aqueous NH_3BH_3 and $NaBH_4$ solution).

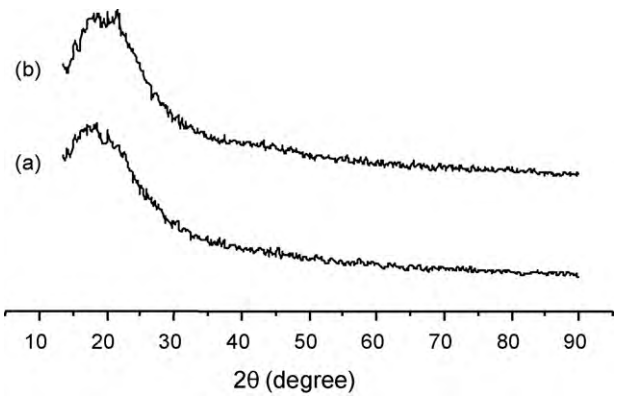

Fig. 3. Powder X-ray diffraction patterns for (a) the Co–SiO_2 nanospheres and (b) the synthesized SiO_2 supported Co catalyst after the hydrolysis of NH_3BH_3.

the catalysts without pretreatment, $NaBH_4$ was mixed with H_2O, NH_3BH_3, and the catalyst. Hydrogen is evolved via following two reactions:

$$NaBH_4 + 2H_2O \rightarrow Na^+ + BO_2^- + 4H_2 \quad (1)$$

$$NH_3BH_3 + 2H_2O \rightarrow NH_4^+ + BO_2^- + 3H_2 \quad (2)$$

Under the present reaction conditions, about 20 mL hydrogen is generated via reaction (1), and about 120 mL of hydrogen is generated via reaction (2). The molar ratio of the hydrolytically generated hydrogen to the initial NH_3BH_3 in the presence of the Co–SiO_2 nanospheres and the SiO_2 supported Co catalyst are ca. 3.0. The

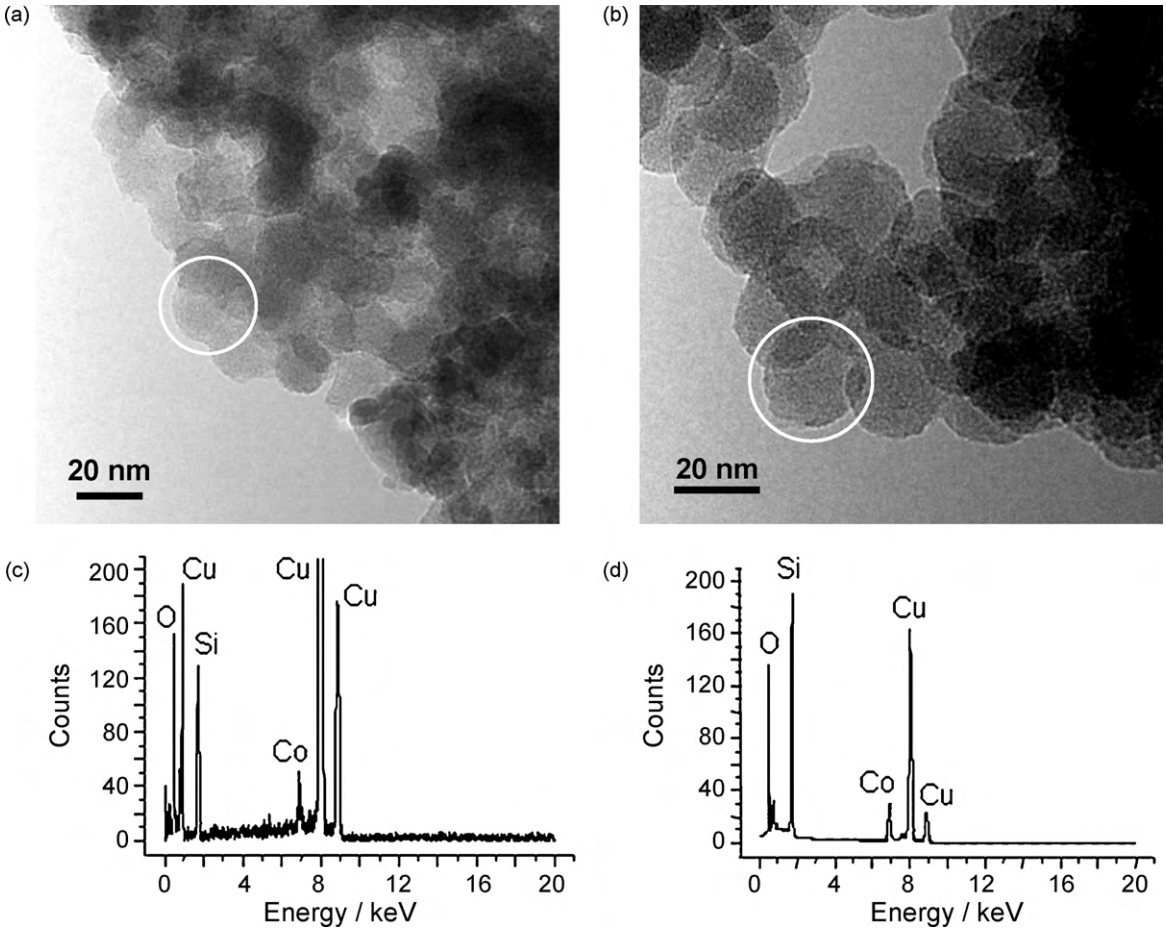

Fig. 4. TEM images of (a) the Co–SiO_2 nanospheres and (b) the SiO_2 supported Co catalyst after the hydrolysis of NH_3BH_3, and the corresponding EDX spectra (c and d).

theoretical molar ratio of the reaction completion is 3.0, thus the results indicate that dehydrogenation is completed in the presence of the Co–SiO_2 nanospheres and the SiO_2 supported Co catalysts. In comparison with the case of the SiO_2 supported Co catalyst, low hydrogen release rate was observed for the Co–SiO_2 nanospheres, suggesting that the reduction of the cobalt species is more difficult in the hollow Co–SiO_2 nanospheres. As shown in Fig. 2, at the 1 cycle of use of the reduced samples, almost the same catalytic activities were observed.

We analyzed the X-ray diffraction patterns of the Co–SiO_2 nanospheres and the SiO_2 supported Co catalysts after the hydrolysis of NH_3BH_3. Both XRD profiles for the Co–SiO_2 nanospheres and the SiO_2 supported Co catalysts show only a broad peak at 2θ = ca. 20°, which is assigned to the amorphous silica, while the profiles show no diffraction line assignable to any cobalt species (Fig. 3). These results indicate that Co particles in both catalysts are amorphous and/or the particle size is too small after the hydrolysis of NH_3BH_3.

The morphologies of the Co–SiO_2 nanospheres and the SiO_2 supported Co catalyst after the hydrolysis of NH_3BH_3 were examined using TEM. The TEM image of the Co–SiO_2 nanospheres shows spherical particles with 15–30 nm diameters (Fig. 4a). The TEM image of the SiO_2 supported Co catalyst also shows spherical particles with 15–30 nm diameters (Fig. 4b). Due to low contrast of the TEM images, we cannot identify the Co particles in both the samples. To confirm the presence of Co, we carried out EDX experiments. Fig. 4c and d shows the EDX spectra of the regions marked in Fig. 3a and b. The EDX spectra exhibits Kα peaks corresponding to O (0.52 keV), Co (6.93 keV), and Si (1.74 keV) elements, and Cu signals (0.93, 8.05, and 8.94 keV) from the TEM grid. The EDX analysis indicates that a particle of the Co–SiO_2 nanospheres and the SiO_2 supported Co catalysts includes Co. For both samples, fine Co

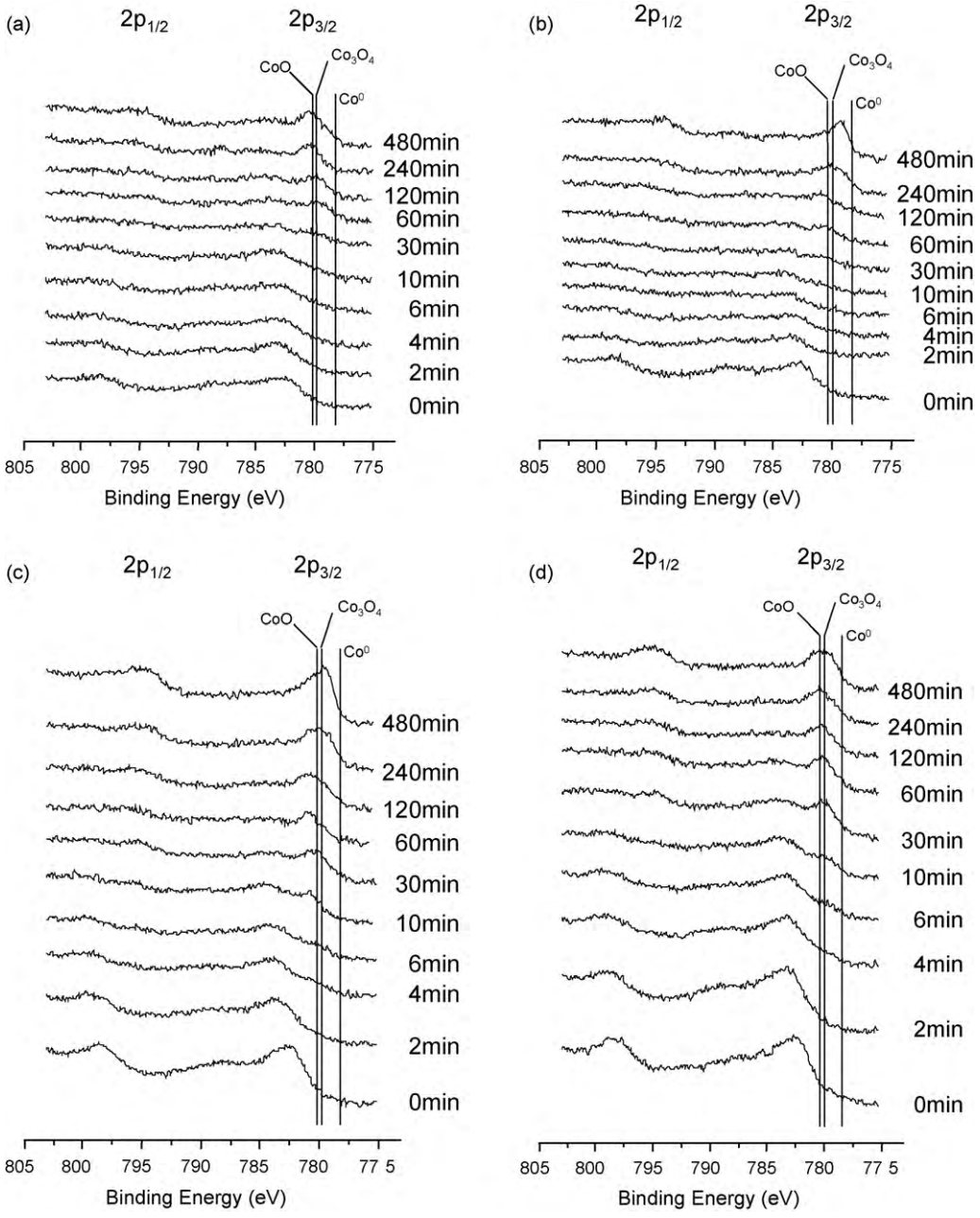

Fig. 5. Co 2p XPS obtained from (a and c) the Co–SiO_2 nanospheres and (b and d) the SiO_2 supported Co catalysts before and after the hydrolysis of NH_3BH_3. The profiles were obtained using 2 keV-Ar^+ sputtering times of 0, 2, 4, 6, 10, 30, 60, 120, 240, and 480 min.

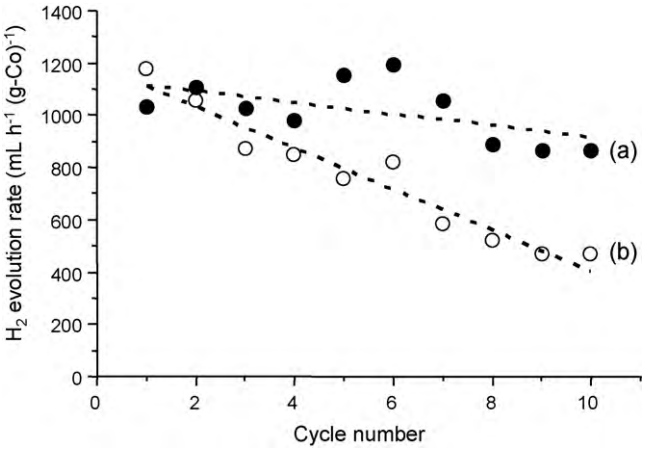

Fig. 6. The hydrogen evolution rates for the uninterrupted cycle of (a) the Co–SiO_2 nanospheres and (b) the SiO_2 supported Co catalyst vs. the cycle number. Co/NH_3BH_3 = 0.05.

particles of ca. 2 nm in diameter rolled around freely inside or on the surface of the SiO_2 nanospheres after electron beam irradiation for a certain period.

We analyzed the X-ray photoelectron spectra (XPS) of the Co–SiO_2 nanospheres after the hydrolysis of NH_3BH_3 in combination with argon ion etching to confirm the presence of Co inside or on the surface of the SiO_2 nanospheres. Fig. 5a shows the Co 2p spectra of the Co–SiO_2 nanosphere surface before and after Ar^+ sputtering. The Co $2p_{3/2}$ and/or Co $2p_{1/2}$ peaks can be observed before and after Ar^+ sputtering in Fig. 5a. It has been reported that the metallic cobalt (Co^0), Co_3O_4, and CoO exhibit Co $2p_{3/2}$ bands at about 778, 779.5, and 780.5 eV, respectively [46–49]. Up to a 10-min sputtering, the spectra exhibit Co $2p_{3/2}$ bands at around 782.5 eV, indicating that Co^{2+} species, for example, cobalt silicate [48,49]. The spectra of the Co–SiO_2 nanospheres after the hydrolysis of NH_3BH_3 up to a 10-min sputtering exhibit a Co $2p_{3/2}$ bands at a similar binding energy (Fig. 5c). The Co $2p_{3/2}$ band around 780.5 eV appeared in the spectra from 30-min through 480-min sputtering, indicating that the Co^{2+} species (CoO or cobalt silicate) is the dominant cobalt species in the Co–SiO_2 nanospheres before the hydrolysis of NH_3BH_3 (Fig. 5a). The spectrum of the Co–SiO_2 nanospheres after the hydrolysis of NH_3BH_3 exhibits a Co $2p_{3/2}$ band at around 779.5 eV with a shoulder at 778–779.5 eV from 30-min through 480-min sputtering (Fig. 5c), indicating that the Co–SiO_2 nanospheres after the hydrolysis of NH_3BH_3 include metallic cobalt species. These results suggest that cobalt species in the Co–SiO_2 nanospheres were reduced during the reaction with $NaBH_4$ and the hydrolysis of NH_3BH_3. Otherwise, the spectrum of the SiO_2 supported Co catalyst exhibit a Co $2p_{3/2}$ band at around 782.5 eV before Ar^+ sputtering (Fig. 5b), which are Co^{2+} species (CoO or cobalt silicate). The spectra of the SiO_2 supported Co catalyst before hydrolysis of NH_3BH_3 exhibit a peak around 779 eV in the spectra from 30-min through 480-min sputtering, indicating that the SiO_2 supported Co catalyst includes metallic cobalt and oxidized cobalt species. The Co $2p_{3/2}$ band of the SiO_2 supported Co catalyst after the hydrolysis of NH_3BH_3 becomes broader at a higher binding energy than the band of the catalyst before the hydrolysis of NH_3BH_3, indicating that some Co species in the SiO_2 supported Co catalyst after hydrolysis of NH_3BH_3 are oxidized after air exposure.

Fig. 6 shows the hydrogen evolution rates for the uninterrupted cycles of the Co catalysts obtained via the reduction in aqueous NH_3BH_3 and $NaBH_4$ solutions. The evolution rates were calculated by averaging the hydrogen amounts evolved every minute in the 5–50% range of the maximum amounts evolved in the presence of each catalyst. For the 1st cycle, both the Co–SiO_2 nanospheres and the SiO_2 supported Co catalyst show almost the same hydrogen evolution rates. The hydrogen evolution rates in the presence of the Co–SiO_2 nanospheres are at almost the same level through 10 cycles. On the other hand, the hydrogen evolution rates in the presence of the SiO_2 supported Co catalysts gradually decrease with the increasing cycle number, and only 39% of the evolution rates for the 1st cycle remained for the 10th cycle in the presence of the SiO_2 supported Co catalyst. These results indicate that the Co–SiO_2 nanospheres show a higher durability than the SiO_2 supported Co catalyst. The hydrogen evolution rate in the presence of the Co–SiO_2 nanospheres for the 10th cycle is 1.9 times higher than that in the presence of the SiO_2 supported Co catalyst.

We analyzed the morphologies of the Co–SiO_2 nanospheres and the SiO_2 supported Co catalyst after 10 cycles using TEM (Fig. 7). The TEM images of the Co–SiO_2 nanospheres and the SiO_2 supported Co catalyst reveal that the morphologies of the catalysts have not changed compared to the morphologies of the catalysts after the first hydrolysis run of NH_3BH_3 (Fig. 4). Both catalysts also had TEM images of low contrast, indicating that cobalt particles in both catalysts still have a cluster size even after 10 cycles.

We analyzed the filtrates after 10 cycles in the presence of the Co–SiO_2 nanospheres and the SiO_2 supported Co catalyst to confirm leaching of the active metal from the catalysts by ICP measurements. The Co contents in the filtrate after the cycling in the presence of the Co–SiO_2 nanospheres is 1.6 mg L^{-1}, while the Co contents in the filtrate after the cycling in the presence of the SiO_2

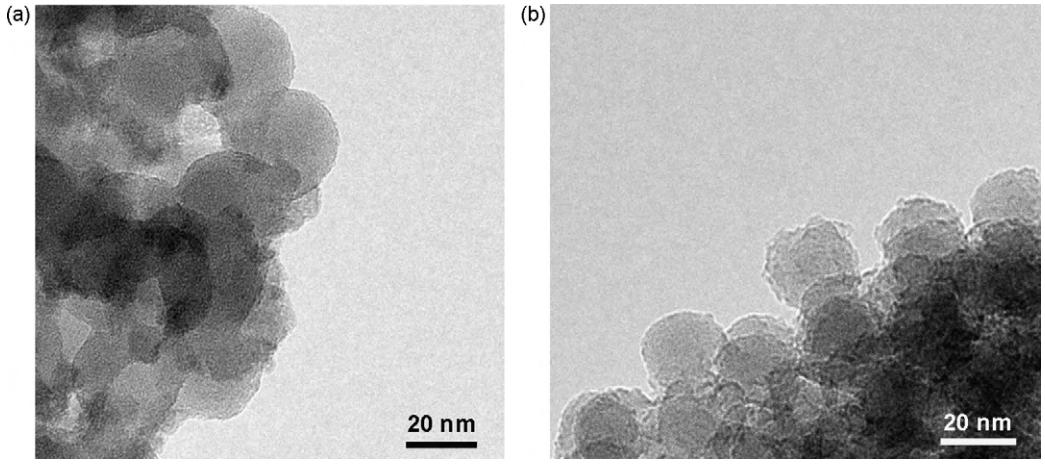

Fig. 7. TEM images of (a) the Co–SiO_2 nanospheres and (b) the SiO_2 supported Co catalyst after 10 cycles.

supported Co catalyst is 4.6 mg L^{-1}. The Co contents in both catalysts used for the cycling tests are 43.1 mg L^{-1}, thus 3.7 and 10.7% Co were leached from the Co–SiO_2 nanospheres and from the SiO_2 supported Co catalyst, respectively. The observation reveals that the leaching amount from the Co–SiO_2 nanospheres during the cycling tests was much lower than that from the SiO_2 supported Co catalyst, reflecting the durability is much higher for the Co–SiO_2 nanospheres than the SiO_2 supported Co catalyst. As shown in Fig. 1, with the un-reduced samples, higher hydrogen evolution rate from the aqueous NH_3BH_3 and $NaBH_4$ solution was observed for the SiO_2 supported Co catalyst than for the Co–SiO_2 nanospheres because the reduction of Co^{2+} to catalytically active Co^0 species was easier for the former than for the latter. At the first cycle of use of the reduced samples, both of the Co–SiO_2 nanospheres and the SiO_2 supported Co catalyst showed almost the same catalytic activity (Fig. 2). However, after several cycles, the Co–SiO_2 nanospheres kept almost its activity while the SiO_2 supported Co catalyst significantly lost its activity (Fig. 6), indicating that the Co–SiO_2 nanospheres have much higher durability. The present results suggest that in comparison with metal-supported catalysts, the protection of catalytically active species with SiO_2 nanospheres could be an effective approach for preparing catalysts with high durability for hydrolysis of ammonia borane.

4. Conclusion

Silica nanospheres (15–30 nm) containing cobalt clusters were synthesized using a $Co(NH_3)_6Cl_3$ crystal template method in a polyoxyethylene-nonylphenyl ether/cyclohexane reversed micelle system followed by in situ reduction in aqueous $NaBH_4/NH_3BH_3$ solutions. Cobalt clusters are located both inside and on the outer surface of the silica nanospheres as shown by the TEM/EDX and XPS measurements. The cobalt–silica nanospheres show a high enough catalytic activity for the hydrolysis of ammonia borane that generates a stoichiometric amount of hydrogen, and can be efficiently cycled and reused 10 times without any significant loss of the catalytic activity.

Acknowledgements

The authors would like to thank NEDO and AIST for their financial support, Dr. Akita and Dr. Uchida for the TEM measurements, and the reviewers for valuable suggestions.

References

[1] L. Schlapbach, A. Züttel, Nature 414 (2001) 353–358.
[2] N.L. Rosi, J. Eckert, M. Eddaoudi, D.T. Vodak, J. Kim, M. O'Keeffe, O.M. Yaghi, Science 300 (2003) 1127–1129.
[3] G.A. Deluga, J.R. Salge, L.D. Schmidt, X.E. Verykios, Science 303 (2004) 993–997.
[4] P. Chen, Z. Xiong, J. Luo, J. Lin, K.L. Tan, Nature 420 (2002) 302–304.
[5] S.C. Amendola, S.L. Sharp-Goldman, M. Saleem Janjua, M.T. Kelly, P.J. Petillo, M. Binder, J. Power Sources 85 (2) (2000) 186–189.
[6] S.C. Amendola, S.L. Sharp-Goldman, M. Saleem Janjua, N.C. Spencer, M.T. Kelly, P.J. Petillo, M. Binder, Int. J. Hydrogen Energy 25 (10) (2000) 969–975.
[7] T. Umegaki, J.-M. Yan, X.-B. Zhang, H. Shioyama, N. Kuriyama, Q. Xu, Int. J. Hydrogen Energy 34 (5) (2009) 2303–2311.
[8] A. Gutowska, L. Li, Y. Shin, C.M. Wang, X.S. Li, J.C. Linehan, R.S. Smith, B.D. Kay, B. Schmid, W. Shaw, M. Gutowski, T. Autrey, Angew. Chem. Int. Ed. 44 (23) (2005) 3578–3582.
[9] M.C. Denney, V. Pons, T.J. Hebden, D. Michael Heinekey, K.I. Goldberg, J. Am. Chem. Soc. 128 (37) (2006) 12048–12049.
[10] R.J. Keaton, J.M. Blacquiere, R. Tom Baker, J. Am. Chem. Soc. 129 (7) (2007) 1844–1845.
[11] M. Chandra, Q. Xu, J. Power Sources 156 (2) (2006) 190–194.
[12] M. Chandra, Q. Xu, J. Power Sources 159 (2) (2006) 855–860.
[13] Q. Xu, M. Chandra, J. Power Sources 163 (1) (2006) 364–370.
[14] M. Chandra, Q. Xu, J. Power Sources 168 (1) (2007) 135–142.
[15] T.J. Clark, G.R. Whittell, I. Manners, Inorg. Chem. 46 (18) (2007) 7522–7527.
[16] P.V. Ramachandran, P.D. Gagare, Inorg. Chem. 46 (19) (2007) 7810–7817.
[17] M. Zahmakıran, S. Özkar, Appl. Catal. B 89 (1–2) (2009) 104–110.
[18] S. Basu, A. Brockman, P. Gagare, Y. Zheng, P.V. Ramachandran, W.N. Delgass, J.P. Gore, J. Power Sources 188 (1) (2009) 238–243.
[19] H.-L. Jiang, S.K. Singh, J.-M. Yan, X.-B. Zhang, Q. Xu, ChemSusChem 3 (5) (2010) 541–549.
[20] J.-M. Yan, X.-B. Zhang, S. Han, H. Shioyama, Q. Xu, Angew. Chem. Int. Ed. 47 (12) (2008) 2287–2289.
[21] C.F. Yao, L. Zhuang, Y.L. Cao, X.P. Ai, H.X. Yang, Int. J. Hydrogen Energy 33 (10) (2008) 2462–2467.
[22] S.B. Kalidindi, M. Indirani, B.R. Jagirdar, Inorg. Chem. 47 (16) (2008) 7424–7429.
[23] S.B. Kalidindi, U. Sanyal, B.R. Jagirdar, Phys. Chem. Chem. Phys. 10 (38) (2008) 5870–5874.
[24] T. Umegaki, J.-M. Yan, X.-B. Zhang, H. Shioyama, N. Kuriyama, Q. Xu, Int. J. Hydrogen Energy 34 (9) (2009) 3816–3822.
[25] T. Umegaki, J.-M. Yan, X.-B. Zhang, H. Shioyama, N. Kuriyama, Q. Xu, J. Power Sources 191 (2) (2009) 209–216.
[26] Ö. Metin, S. Özkar, Energy Fuels 23 (7) (2009) 3517–3526.
[27] J.-M. Yan, X.-B. Zhang, S. Han, H. Shioyama, Q. Xu, Inorg. Chem. 48 (15) (2009) 7389–7393.
[28] F. Durap, M. Zahmakıran, S. Özkar, Int. J. Hydrogen Energy 34 (17) (2009) 7223–7230.
[29] J.-M. Yan, X.-B. Zhang, S. Han, H. Shioyama, Q. Xu, J. Power Sources 194 (1) (2009) 478–481.
[30] J.-M. Yan, X.-B. Zhang, H. Shioyama, Q. Xu, J. Power Sources 195 (4) (2009) 1091–1094.
[31] H.-L. Jiang, T. Umegaki, T. Akita, X.-B. Zhang, M. Haruta, Q. Xu, Chem. Eur. J. 16 (10) (2010) 3132–3137.
[32] M. Giersig, T. Ung, T.M. Liz-Marzán, P. Mulvaney, Adv. Mater. 9 (7) (1997) 570–575.
[33] W. Wang, S.A. Asher, J. Am. Chem. Soc. 123 (50) (2001) 12528–12535.
[34] T. Torimoto, J. Paz Reyes, K. Iwasaki, B. Pal, T. Shibayama, K. Sugawara, H. Takahashi, B. Ohtani, J. Am. Chem. Soc. 125 (2) (2003) 316–317.
[35] Y. Yang, M. Gao, Adv. Mater. 17 (19) (2005) 2354–2357.
[36] Y. Yang, L. Jing, X. Yu, D. Yan, M. Gao, Chem. Mater. 19 (17) (2007) 4123–4128.
[37] T. Haeiwa, K. Segawa, K. Konishi, J. Magn. Magn. Mater. 310 (2) (2007) e809–e811.
[38] T. Miyao, N. Toyoizumi, S. Okuda, Y. Imai, K. Tajima, S. Naito, Chem. Lett. 28 (10) (1999) 1125–1126.
[39] A.J. Zarur, J.Y. Ying, Nature 403 (2000) 65–67.
[40] M. Ikeda, M. Tago, M. Kishida, M. Wakabayashi, Chem. Commun. (23) (2001) 2512–2513.
[41] S. Takenaka, K. Hori, H. Matsune, M. Kishida, Chem. Lett. 34 (12) (2005) 1594–1595.
[42] S. Takenaka, H. Umebayashi, E. Tanabe, H. Matsune, M. Kishida, J. Catal. 245 (2) (2007) 392–400.
[43] T. Miyao, K. Minoshima, S. Naito, J. Mater. Chem. 15 (23) (2005) 2268–2270.
[44] S. Naito, K. Minoshima, T. Miyao, Top. Catal. 39 (3–4) (2006) 131–136.
[45] T. Miyao, K. Minoshima, Y. Kurokawa, K. Shinohara, W. Shen, S. Naito, Catal. Today 132 (1–4) (2008) 132–137.
[46] B. Ernst, S. Libs, P. Chaumette, A. Kiennemann, Appl. Catal. A 186 (1–2) (1999) 145–168.
[47] Q. Tang, Q. Zhang, P. Wang, Y. Wang, H. Wan, Chem. Mater. 16 (10) (2004) 1967–1976.
[48] A.Y. Khodakov, A. Griboval-Constant, R. Bechara, V.L. Zholobenko, J. Catal. 206 (2) (2002) 230–241.
[49] C. Chupin, A.C. van Veen, M. Konduru, J. Després, C. Mirodatos, J. Catal. 241 (1) (2006) 103–114.